The Report Committee for Jennifer Yvonne Kaser
Certifies that this is the approved version of the following report:

Utilizing Natural Scene Statistics and Blind Image Quality Analysis of Infrared Imagery

APPROVED BY
SUPERVISING COMMITTEE:

Supervisor:

Alan Bovik

Christine Julian

Utilizing Natural Scene Statistics and Blind Image Quality Analysis of Infrared Imagery

by

Jennifer Yvonne Kaser, B.S.

Report

Presented to the Faculty of the Graduate School of

The University of Texas at Austin

in Partial Fulfillment

of the Requirements

for the Degree of

Master of Science in Engineering

The University of Texas at Austin

August 2013

Abstract

Utilizing Natural Scene Statistics and Blind Image Quality Analysis of Infrared Imagery

Jennifer Yvonne Kaser, M.S.E.

The University of Texas at Austin, 2013

Supervisor: Alan Bovik

With the increasing number and affordability of image capture devices, there is an increasing demand to objectively analyze and compare the quality of images. Image quality can also be used as an indicator to determine if the source image is of high enough quality to perform analysis on. When applied to real world scenarios, use of a blind algorithm is essential since a flawless reference image typically is unavailable. Recent research has shown promising results in no reference image quality utilizing natural scene statistics in the visual image space. Research has also shown that although the statistical profiles vary slightly, there are statistical regularities in IR images as well which would indicate that natural scene statistical models may be able to be applied. In this project, I will analyze BRISQUE quality features of IR images and determine if the algorithm can successfully be applied to IR images. Additionally, in order to validate the usefulness of these techniques, the BRISQUE quality features are analyzed using a detection algorithm to determine if they can be used to predict conditions which may cause missed detections.

Table of Contents

List of Tables

List of Figures

Chapter 1

Introduction

The ability to see the unseen is a valuable capability which has led to the development of various sensors to detect light outside the visible spectrum such as infrared thermal imagery. These sensors can be invaluable in applications utilizing them for detecting various objects such as pedestrians at night, identifying humans in low visibility situations in a fiery building, and various other tactical situations. Utilization of these technologies and algorithms effectively can improve performance of the task at hand and in certain situations even lead to lives saved.

The quality of the images used for tasks and analysis can have a significant impact on task and algorithm performance. Development in analyzing images for quality in the visible spectrum has been driven by the increasing number and affordability of visual image capture devices. When evaluating quality, if an algorithm does not use the original pristine reference image or information, an algorithm is said to be blind or no-reference. Recent research has shown promising results in no reference image quality utilizing natural scene statistics in the visual image space to determine overall image quality independent of the distortion (BRISQUE) [1]. Research has also shown that although the statistical profiles vary slightly, there are statistical regularities in IR images as well which would indicate that natural scene statistical models may be able to be applied [2].

In this project, I will analyze the natural scene statistics of IR images and determine if blind image quality algorithms utilizing natural scene statistics in the visual space can be applied to IR images and what additional adjustments may be necessary. Image quality can also be used as an indicator to determine if the source image is of high

enough quality to perform analysis or as an input to an algorithm to determine confidence of detection [3]. In most infrared image applications, perceived quality from a human is not necessarily as important as ensuring the quality of the image is high enough to perform the desired task [4]. Therefore, in order to validate the usefulness of these techniques I will incorporate use of the image quality features utilized for the BRISQUE algorithm along with a detection algorithm which uses both visual and infrared imagery and analyze if there is correlation between the quality features and false negatives.

Chapter 2

Background

Operating in wavelengths from 700 nm to 1 mm, infrared imaging cameras capture images which emit thermal radiation. They are utilized in multiple applications such as night vision cameras, various industrial applications, scientific imaging in astronomy, and medical imaging. Each pixel represents a specific temperature value. Depending on the application, these temperatures can be mapped either to a color or grayscale image. In this section I review previous research in the area of analyzing infrared imagery as well as work that has been done in quality analysis of imagery. Finally, I will survey what has been done in applying quality metrics to detection algorithms in infrared imagery. In this report I will be analyzing gray scale infrared images from both indoor and outdoor scenes such as the one shown in Figure 1.

Figure 1: Example of Grayscale Infrared Image.

IMAGE QUALITY

Image Quality Analysis (IQA) falls into several different categories depending on the need for additional information with the image to be analyzed. Full reference algorithms require a pristine image without defects to compare against in order to evaluate the quality of the image. Reduced reference images also require some knowledge about the original image but not necessarily the full reference image [5]. Since in most infrared applications, reference image information is not available, these types of algorithms will not be considered or evaluated.

As images have been more extensively studied and computation has become more accessible, research in the area of image analysis has grown. Research has shown that natural images, non-computer generated images, have certain statistical properties which hold across all image types, regardless of what the image captures [6]. In the visual image space, these properties have been shown to translate to measures of human perceptual image quality [7-10].

Tang *et. al.* [7] proposed a blind image quality algorithm called LBIQ. This is an algorithm which was proven useful in the visual image space and utilizes features in the wavelet domain to capture image features utilizing natural scene statistics to evaluate presence of multiple distortions such as texture, blur and noise. It utilizes a machine learning algorithm in order to calculate an image quality score. This algorithm has promising results; however it requires a transform to be done in the wavelet domain which is computationally complex when running on an embedded real time system.

Peng *et. al.* [8] also contributed with a multi-distortion blind image quality algorithm based on using Gabor feature vectors and utilizing a codebook lookup to determine the quality of an image. It also incorporates machine learning methods into the algorithm to predict quality. For this approach the complexity of the calculations was

high, however the author noted it could be optimized by utilizing parallel programming techniques since calculations were independent.

BLIINDS-II proposed by Saad *et. al.* [9] is another blind image quality algorithm which utilizes discrete cosine transform coefficients as quality features in order to predict human perceptual quality of an image. This algorithm also requires a transformation that is more computationally intensive and not applicable in a real-time environment.

Moorthy *et. al.* [10] proposed utilizing wavelet coefficients an algorithm called DIIVINE which also utilizes wavelet coefficients and a trained set of images with distortions to calculate a total of 88 quality features. This algorithm is computationally complex taking 60 seconds to analyze an image and not applicable to a real-time application.

One such algorithm which has shown promising results in the visual image space without requiring transformations is BRISQUE. This algorithm is a No-reference image quality algorithm which does not require any image transformations making it less computationally complex than other algorithms. It is based on the regularity of utilizing natural scene statistics to determine if there are image defects which degrade the quality of images [11]. Unlike other approaches which detect a single type of image defect [12-13], this one doesn't look for specific types of quality issues but evaluates the entire image for multiple types of image defects. The algorithm uses a set of 36 features in order to identify different distortions in the images [1]. Due to the robustness of identifying many different image defects without a reference image and its potential to be applied to real-time imaging applications, this is the algorithm which was chosen for evaluation in the infrared image space. Although it has yet to be applied to infrared imagery, the statistical profiles of infrared images seem to be similar to images in the visual space as described in the following sections.

IMAGE QUALITY IN INFRARED IMAGES

In infrared imagery, there are two major factors that typically inhibit the imagery from being the most useful due to sensor limitations and physical characteristics of heat; noise and low contrast levels. This has led to preprocessing of imagery often in hardware in order to improve the quality and utility of the images utilizing different methods such as variants of histogram equalization and utilization of principal components analysis [14-16]. Although these papers provide algorithms which enhance the quality perceived of the image, the results were left to human perception to evaluate the improvement due to the algorithm.

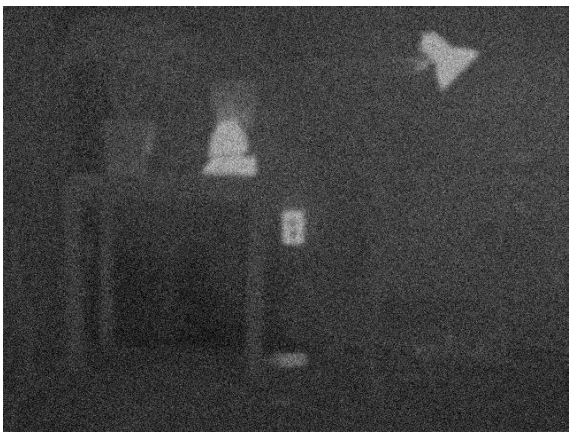

Figure 2: Example of Infrared Image with Noise and Low Contrast.

An early image quality scale for infrared imagery was the National Imagery Interpretability Rating Scale (NIIRS). This scale was defined as a number from 0 to 9 which defined the level of detail that the image could contain. Each level has a qualitative description used to evaluate the imagery [17]. This scale requires a human to evaluate the image to determine which level that the image falls into. Also, many of the descriptions of the levels seem to be targeted toward certain applications which may make certain images difficult to analyze.

Since infrared images are typically used for a specific task purpose, Rouse and Hemami describe a method to measure perceived utility of images (NICE). This algorithm utilizes image contours to calculate and predict image utility [18]. This paper makes a unique distinction between image quality and image utility and suggests that image utility is more important with certain imaging applications such as infrared images. The limitation of this approach is that requires a reference image to be able to identify image contours.

Zang *et. al.* [19] proposed an infrared quality assessment method based on fractal dimensions. This approach is limited in that it is a partial reference algorithm depending on fractal information from a reference image for comparison.

Long and Li [20] proposed a quality assessment algorithm for assessing quality of infrared facial images in a video sequence. Although the algorithm incorporates some general quality metrics related to blur and darkness, this algorithm is very specific to facial images as it incorporates things like facial tilt and is not generally applicable.

It doesn't appear that to date, any applications of general no reference image quality metrics have been applied to infrared images to enhance task or algorithm performance. Most applications of applying metrics are very specific to the task they are applied to.

DIFFERENCES OF INFRARED AND VISUAL IMAGES

Work by Morris *et. al* [2] compared the image statistics from equivalent infrared and visual images to compare the statistics of properties from each. They found that there are slight differences in the power spectra statistics for infrared images, due to lack of texture, however they propose that there is high application of utilizing natural scene

statistics. Other differences of note include smaller wavelet coefficients when analyzing joint distributions likely due to lower contrast in IR images. Due to these differences, the same regression model and quality weights used to determine score in images in the visual space can't be applied. However, it appears that the same methods could be applied with an infrared imagery database and produce similar results with predicting image quality.

UTILIZING QUALITY METRICS IN DETECTION ALGORITHMS

Although there doesn't appear to be very much research on general quality assessment algorithms for infrared images, there is more research on applying quality measures or metrics to improve algorithm performance.

Daio *et. al* [21] proposed two metrics specifically targeted toward evaluating quality of the image before and after post processing to evaluate the effectiveness in improving the image for detections. These metrics are mainly focused on the target detection action, for example the potential false target number is specifically related to target detection.

Wang *et. al* [22] proposed using target local salient metric (LSM) and global salient metric (GSM) as quality indexes to improve gray scale template matching. Again, these are very specific metrics targeted toward the specific target detection metric and do not represent overall image quality.

Chen *et. al* [23] proposed utilizing different metrics for use in improving Automatic Target Recognition (ATR) performance. They used five different types of metrics and determined that Shift Invariant Discrete Wavelet Transform and the Laplacian pyramid fusion schemes performed best to improve the detection rate of the

images. They propose that multiple metrics are necessary to fully indicate failure of the ATR algorithm, suggesting five which account for 60% of variability. Further research can be done to find a larger set which may cover a larger subset of variability. Since BRISQUE utilizes thirty six features which span multiple image distortions, this may be a good candidate to determine if additional metrics can improve performance even more and add value.

Chapter 3

Research Completed

Research for this project consists of two main parts. The first is to analyze the BRISQUE features for infrared images and compare them against images in the visual space. This will give insight into how well the model can be applied to the infrared space. The second part of this project involves incorporation of the algorithm into as applied to an existing target detection algorithm. In order to validate the utility of the algorithm in the infrared image space, I will use it as a predictor for false negative target detections. Since the algorithm chosen utilizes both visual and infrared images, I will analyze the imagery with visual and infrared features individually as well as both combined to determine which set of features is most useful for prediction.

IMAGE ACQUISITION

Infrared imagery used for initial image quality analysis was gathered from a variety of sources and imaging devices. There is a combination of both outdoor imagery as well as indoor. All outdoor imagery was taken with various Long Wave Infrared (LWIR) imaging units. A total of 37 outdoor images were used. Outdoor image resolution was 640x480 and some of the imagery had post processing algorithms applied to the raw data. A total of 179 indoor images were used. All indoor imagery was taken with Forward Looking Infrared (FLIR) cameras. Indoor imagery also had a resolution of 640x480.

Imagery used for use in target prediction algorithm was visual and infrared. Infrared imagery was taken from Mid-range Wavelength Infrared (MWIR) imaging units and visual and infrared images were utilized to detect objects of interest. A total of 424

image scenes of detections and false detections were used. 75 scenes contained missed detections. Resolution of the images was 640x480.

COMPARING BRISQUE FEATURES

BRISQUE uses a total of 36 features to predict image quality. These features are visualized with a variety of different plots. In the BRISQUE paper, the MSCN distribution plot fitted to a Gaussian is one of the first used to demonstrate that distortions affect the regularity and fit of the mean subtracted contrast normalized (MSCN) coefficients plot. First I compare sample infrared images to see if the MSCN plots share similar properties. The sample infrared image for this example is an outdoor infrared image which has good contrast, low noise and low blur. My hypothesis is that the features and plots for visual images will be similar to infrared images since they share some of the same statistical properties. Since the computation of the MSCN coefficients focuses on local high contrast or object boundaries, the BRISQUE algorithm should be largely unaffected by differences in textures between infrared and visual imagery.

The images used for comparison are shown in Figure 3 along with the plots of their MSCN coefficients. It is easily seen that the MSCN coefficient plots are very similar in nature in that in both images similar features are highlighted.

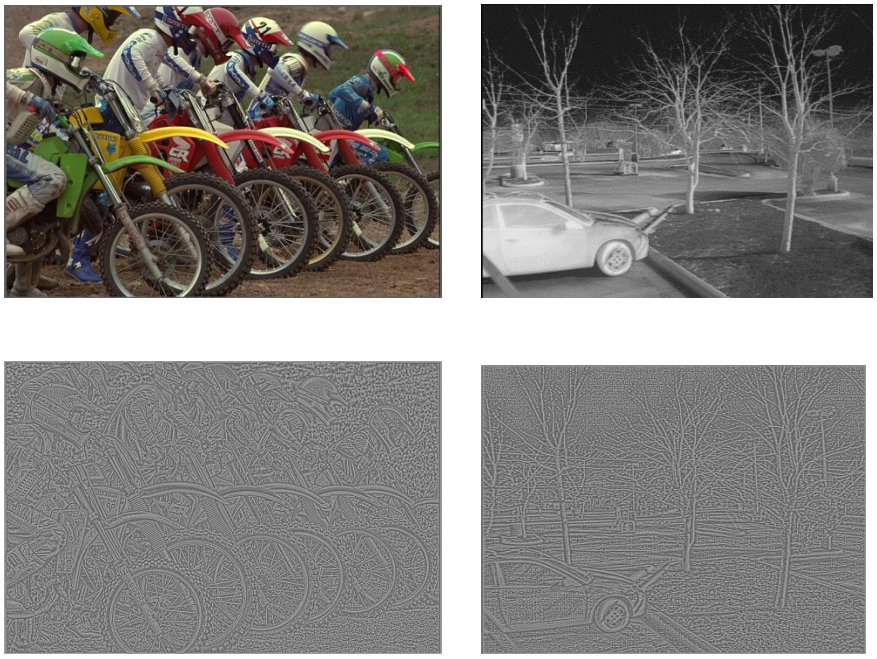

Figure 3: Top Left - Visual Motorcycle Image, Top Right - Infrared Outdoor Image, Bottom Images - MSCN coefficients

In plotting the MSCN distributions, they both appear to be Gaussian in shape and also have similar shape parameters. This is a very important observation as it will enable use of the same methods and calculations that the BRISQUE algorithm uses in order to calculate the first two features since they are based on a generalized Gaussian distribution (GDD) fit.

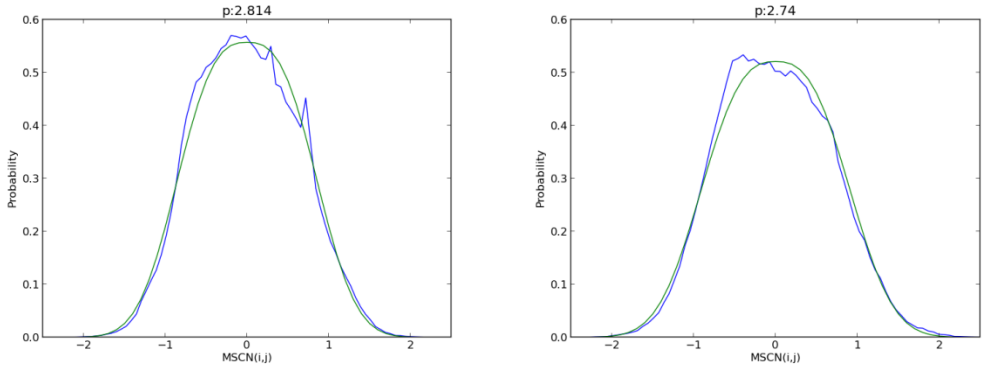

Figure 4: Left – MSCN Distribution Motorcycle Image, Top Right - MSCN Distribution Infrared Outdoor Image

For the remainder of the features, the statistical relationship between neighboring pixels is used. When comparing the scatter plots of both the luminance coefficients and the MSCN coefficients, I expect to see similar results in the plots. Figures 5-8 show scatter plots of both the visual and infrared image for neighboring pixels in different orientations. They appear to have similar shape, however the infrared images have slightly less spread along the diagonal. A noticeable feature in the infrared plots is that there are small vertical and horizontal bands which spread from the lower left corner of the plot. This was present in all sample outdoor images which were taken with different sources but the same system. This feature did not show up in the indoor images so it is likely a side effect of the image acquisition system. This also could be due to the higher number of pixels in the IR images which transition from low levels to higher levels in the image. Zooming in close to the image, in the trees there are many pixels from the branches which have this characteristic. Another notable difference is in the scatter plots of the MSCN coefficients. They seem to be a little less regular in shape than the visual images' scatter plots and have more of a starburst type shape.

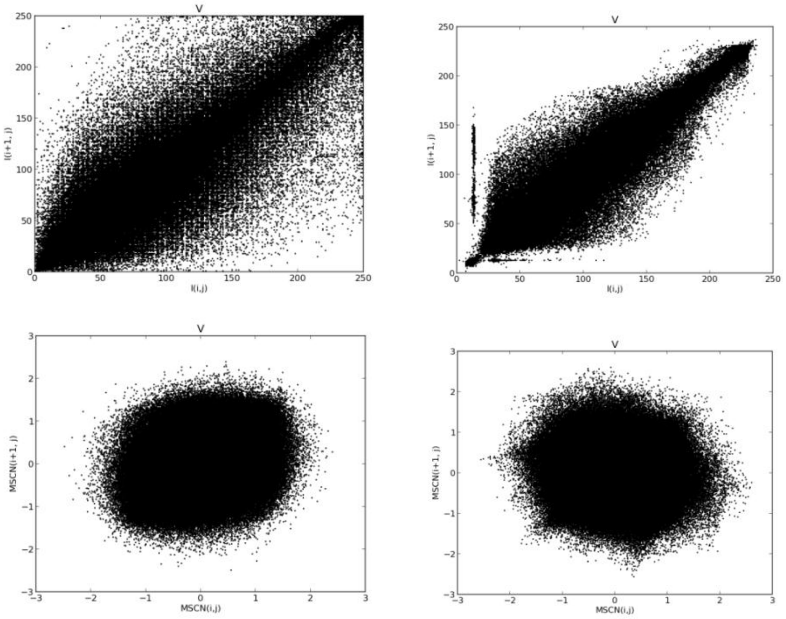

Figure 5: Scatter Plots of Neighboring Values on Vertical Axis. Top – Original Luminance Coefficients, Bottom – MSCN Coefficients, Left – Visual Motorcycle Image, Right – Infrared Outdoor Image

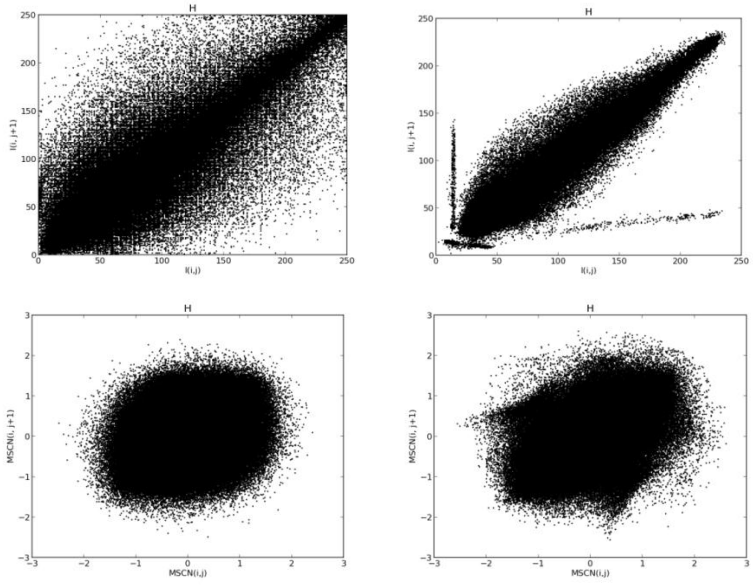

Figure 6: Scatter Plots of Neighboring Values on Horizontal Axis. Top – Original Luminance Coefficients, Bottom – MSCN Coefficients, Left – Visual Motorcycle Image, Right – Infrared Outdoor Image

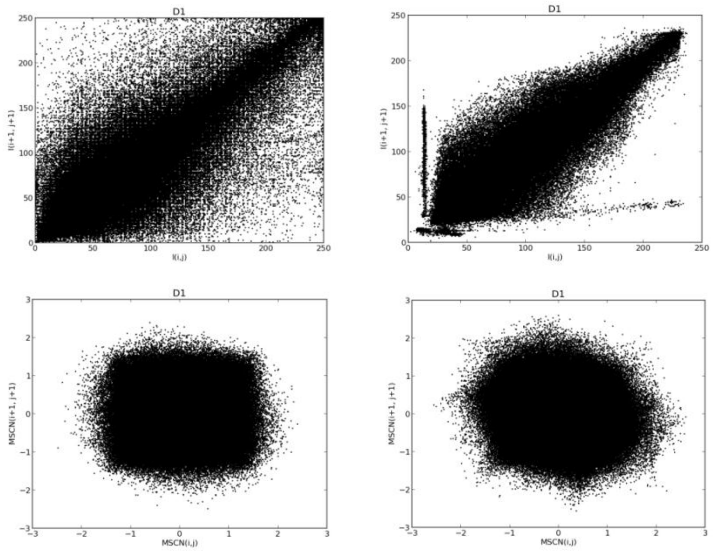

Figure 7: Scatter Plots of Neighboring Values on Main Diagonal Axis. Top – Original Luminance Coefficients, Bottom – MSCN Coefficients, Left – Visual Motorcycle Image, Right – Infrared Outdoor Image

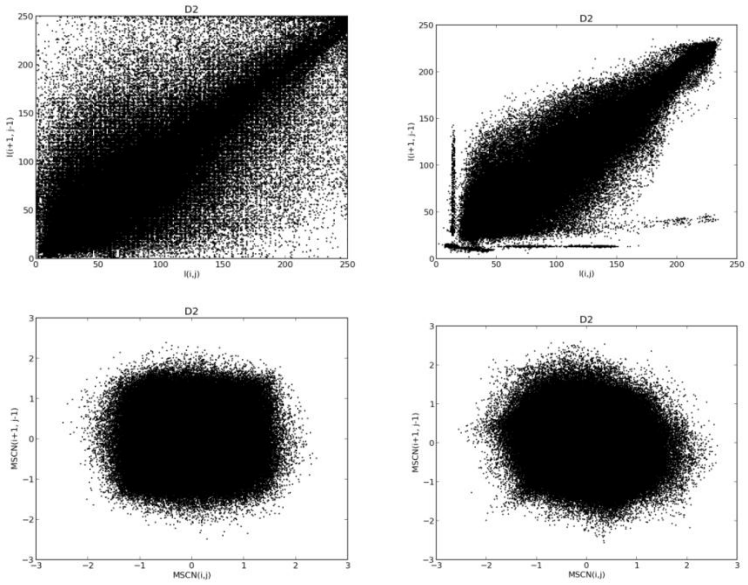

Figure 8: Scatter Plots of Neighboring Values on Secondary Diagonal Axis. Top – Original Luminance Coefficients, Bottom – MSCN Coefficients, Left – Visual Motorcycle Image, Right – Infrared Outdoor Image

COMPARING INDOOR VS. OUTDOOR IMAGES

Visual evaluation of infrared images reveals differences in indoor and outdoor scenes. This is due to less thermal variation in indoor conditions and therefore there is typically less contrast in indoor scenes. Another noticeable difference is objects which have a high temperature tend to be over exposed in the image. In the following figures I will compare a representative indoor infrared image to an outdoor infrared and a visual image to show the statistical similarities and differences.

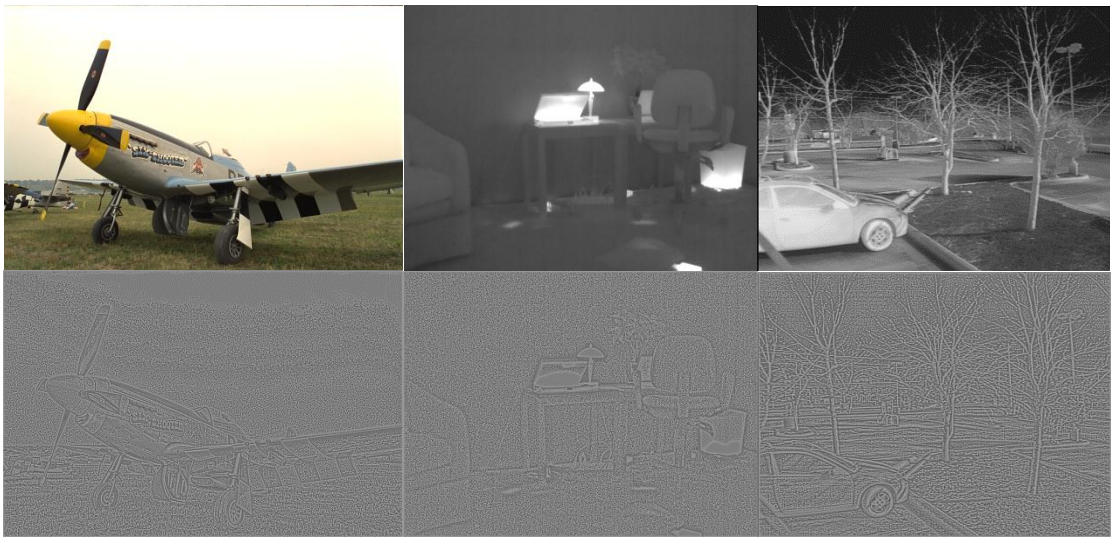

Figure 9: Top Left - Visual Plane Image, Middle - Infrared Indoor Image, Top Right - Infrared Outdoor Image, Bottom Images - MSCN Coefficients

The MSCN distribution in Figure 10 again for the indoor images exhibits a Gaussian distribution. One notable difference in many of the indoor images is that there is a spike near the middle. This is likely due to the concentrated areas of similar high value pixels in the image. In this case the light and the laptop cause that effect. I was able to find a similar effect in one of the visual images. This particular visual image had a large light sky area which caused the spike in the distribution. Another difference

between the indoor and outdoor images to note is that the average shape parameter of the Gaussians between indoor and outdoor images is slightly lower on average. This is likely due to lower contrast in the images.

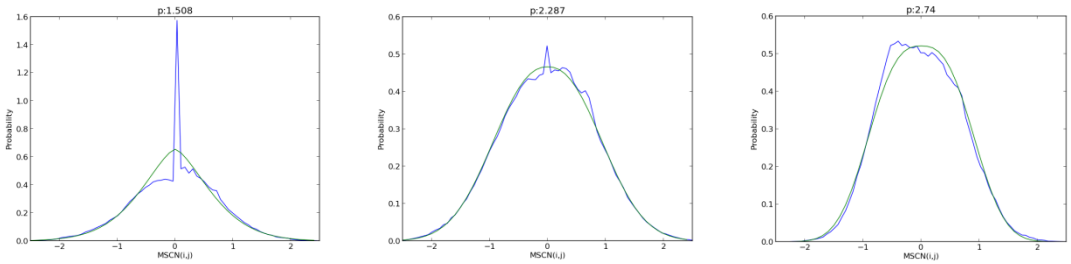

Figure 10: Left – MSCN Distribution Plane Image, Middle - MSCN Distribution Infrared Indoor Image, Right - MSCN Distribution Infrared Outdoor Image

The scatter plots shown in Figures 11-14 show some differences. The luminance scatter plots of the indoor images are much narrower in shape. Visually the indoor images don't utilize the full range of values which can also be shown by the lack of pixels in the lower left hand corner of the plot. For the MSCN scatter plot distributions the indoor images are virtually the same for all orientations in most of the indoor images. They are all very oval in shape. As compared to the visual images, the shape has about the same size with most of the pixels concentrated around a large center.

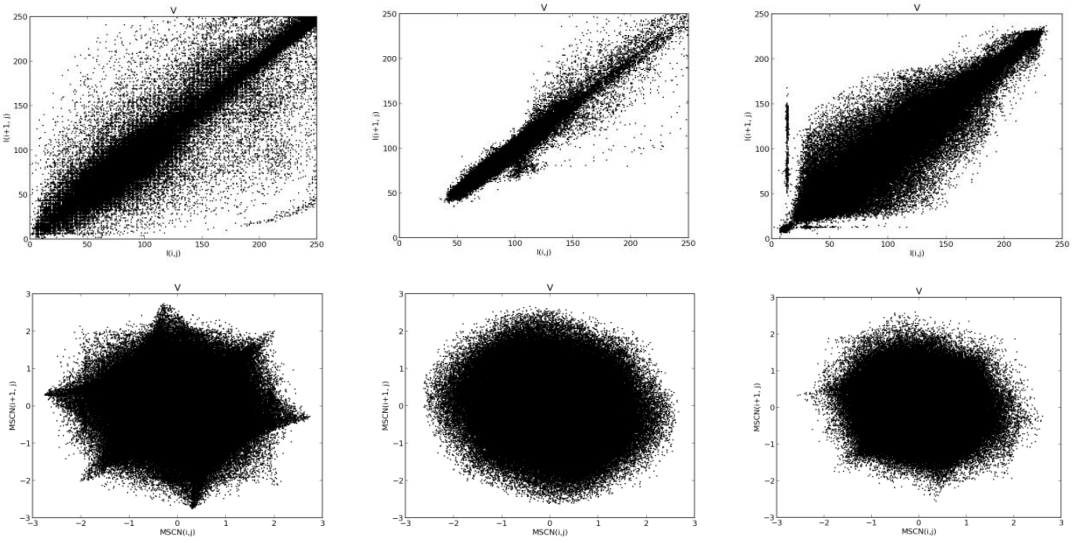

Figure 11: Scatter Plots of Neighboring Values on Vertical Axis. Top – Original Luminance Coefficients, Bottom – MSCN Coefficients, Left – Visual Motorcycle Image, Middle – Indoor Infrared Image, Right – Infrared Outdoor Image

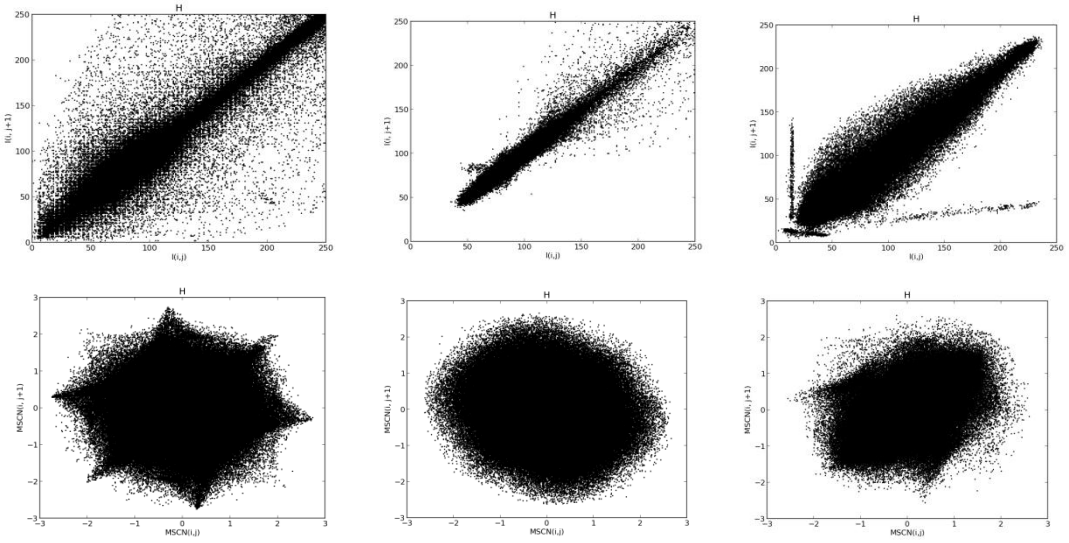

Figure 12: Scatter Plots of Neighboring Values on Horizontal Axis. Top – Original Luminance Coefficients, Bottom – MSCN Coefficients, Left – Visual Motorcycle Image, Middle – Indoor Infrared Image, Right – Infrared Outdoor Image

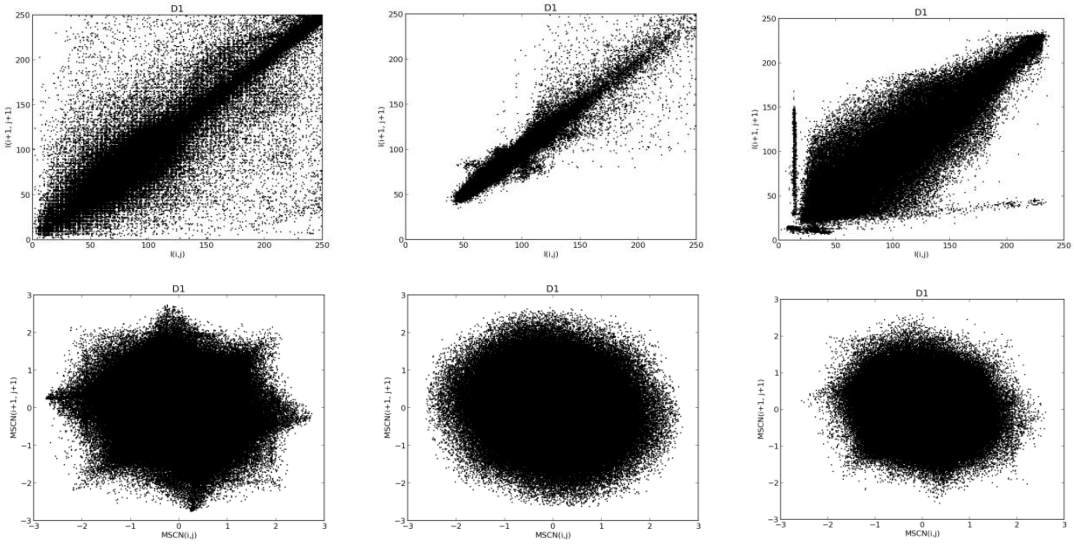

Figure 13: Scatter Plots of Neighboring Values on Main Diagonal Axis. Top – Original Luminance Coefficients, Bottom – MSCN Coefficients, Left – Visual Motorcycle Image, Middle – Indoor Infrared Image, Right – Infrared Outdoor Image

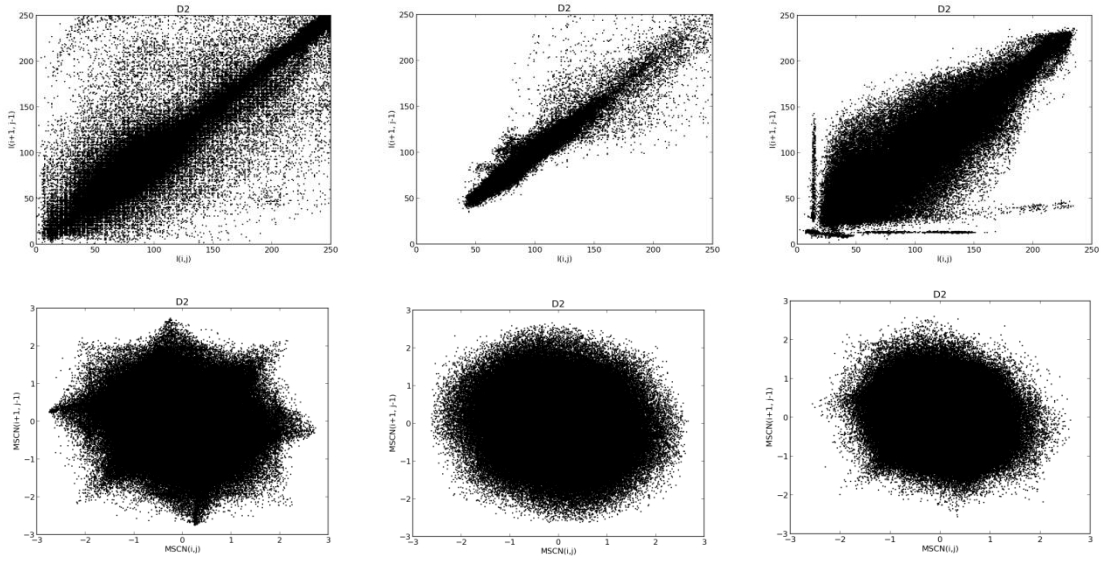

Figure 14: Scatter Plots of Neighboring Values on Secondary Diagonal Axis. Top – Original Luminance Coefficients, Bottom – MSCN Coefficients, Left – Visual Motorcycle Image, Middle – Indoor Infrared Image, Right – Infrared Outdoor Image

INDICATION OF DISTORTIONS IN INFRARED IMAGERY

Another important aspect to analyze is the impact of distortions in the image and the differences in the natural scene statistics and BRISQUE quality features. The indoor image set has a variety of images captured with different distortions present from injecting image defects. The distributions are overlaid to show that the scene statistics are distorted by the different image manipulations. Figures 15-17 show some of the different distorted infrared images which will be used in analysis.

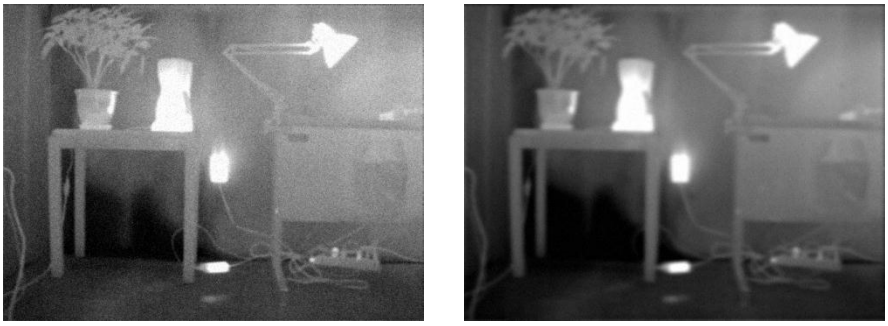

Figure 15: Blur & Noise Distorted Infrared Image

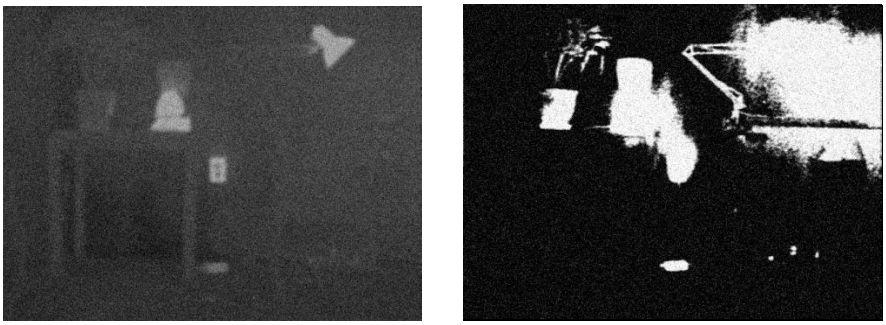

Figure 16: Low and High Contrast Distorted Infrared Image

Figure 17: Original Infrared Image

VALIDATION OF MODEL

In order to validate the utility of quality metrics in a real world application, I will be utilizing over water imagery used for detection of watercraft. The algorithm uses both visual and infrared imagery for detections. An example of the imagery is shown in Figure 18. Under certain environmental conditions the algorithm does not perform as well causing missed detections, example shown in Figure 19. The visual and infrared imagery did have some overlays which were not removed prior to processing since they were constant across all images.

Figure 18: Example Visual and Infrared Images with Detection

Figure 19: Example Visual and Infrared Images with Missed Detection

In this application, I utilize the imagery, infrared and visual quality metrics, and the truth data from the detections to see if there is correlation between the quality features and missed detections. I hypothesize that there will be a correlation between the BRISQUE image features and missed detections and that information can be used to predict conditions where missed targets are likely. If the data shows correlation, it will be possible to put the BRISQUE quality features through a SVM regression model in order to predict when poor image quality may cause missed detections. This regression can be ran with only infrared imagery, only visual imagery and both to determine if performance is better when utilizing quality metrics in the infrared or visual space are more valuable in this application. Since the algorithm utilizes both visual and infrared, I predict that using both sets of quality metrics, totaling 72 features will provide better prediction performance.

Chapter 4

Results

Analysis of BRISQUE Quality Features

In my analysis of the BRISQUE quality features, both infrared and visual imagery had a Gaussian distribution for the MSCN coefficients suggesting that these quality features can be used to characterize infrared imagery similar to visual images. Table 1 quantifies the fit and independence of the MSCN coefficients. The Jarque-Bara (JB) test was used to calculate the goodness of fit to the Gaussian for the image; smaller numbers signify a better fit. As seen qualitatively in the graphs the IR and visual images both fit the Gaussian distribution fairly well when distortions are not present. The visual image of the plane had a very large spike in the MSCN distribution which impacted the Gaussian fit and this is reflected in the large JB coefficient number. Also, Pearson's Chi-Squared test was used to test for independence of the MSCN coefficient values. In all images, the p-value was small on the magnitude of 10^{-3} for all images indicating that the field of values is independent.

Image	JB of MSCN	Chi-Squared	Chi-Squared p-value
Visual Image - Bikes	10.52	3249907.82	9.115 E -3
IR Image – Outdoor	10.35	2720570.40	7.687 E -3
Visual Image – Plane	738.42	3493911.28	5.208 E -3
IR Image Indoor	8.88	3661147.58	6.339 E -3

Table 1: Fit and Independence for Sample Visual and IR Images

Further analysis was done on the set of images gathered to determine the goodness of fit for the images gathered and check for independence. All images showed independence and the results from running the JB goodness of fit calculation is summarized in Table 2. Figure 20 contains sample images which had poor goodness of fit scores, a high JB score, and were outliers in the data set. As can be seen, the IR images have poor contrast and do not have very high quality perceptually. These images are outliers in the set. The indoor image set had a higher number of images with poor contrast and low definition because indoor infrared images typically exhibit these properties due to lower temperature variations.

Image	Number of images	Average JB of MSCN	Median JB of MSCN	Min JB of MSCN	Max JB of MSCN
Visual Reference Images	29	35.04	9.90	9.13	738.42
Outdoor IR	37	16.95	9.55	7.97	149.24
Indoor IR	180	264.10	8.69	6.16	14909.79

Table 2: Average Fit for Sample Visual and IR Images

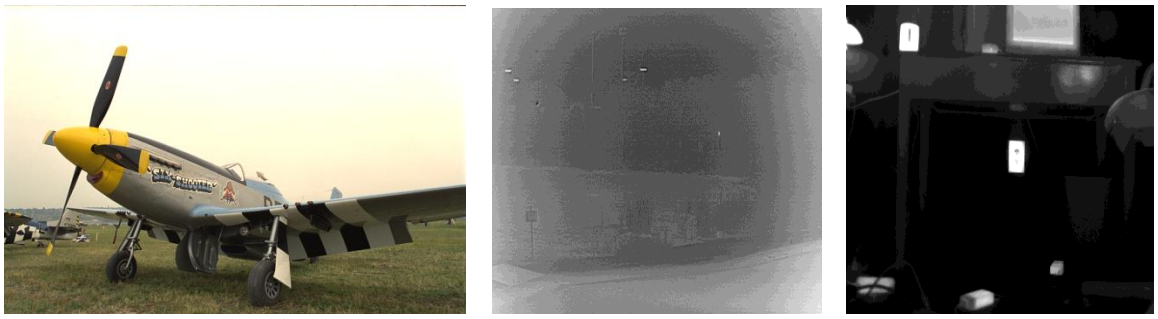

Figure 20: Sample Images with Poor Goodness of Fit Scores (Visual, Outdoor IR, Indoor IR)

The scatter plots of MSCN and luminance coefficients were slightly different between the visual and infrared space. Although slightly different between the modalities, they generally were consistent within the infrared image space. The indoor imagery and the outdoor imagery had different characteristics as well. Due to these slight variations, depending on the application, use of the quality features in indoor and outdoor imagery may have to be utilized differently. Finally, in analyzing the infrared imagery, it was demonstrated that similar to visual images, distortions in the imagery to impact the regularity of the image statistics.

Similar to visual images as demonstrated in the BRISQUE paper. In Figure 21, the distortions to the image show variances from the original image in their MSCN plot of the Gaussian distribution. The differences in shape of the Gaussian do not share as much variation as shown in the BRISQUE report. This could be due to using more highly distorted images to graph. For this example, I chose distortions which still closely mirrored the original image and therefore the differences in the MSCN plots are not drastically different for some distortions.

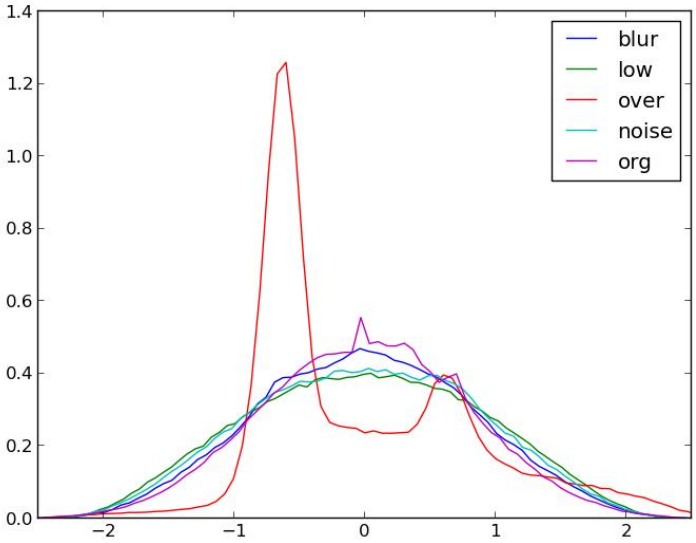

Figure 21: MSCN plots of Indoor Infrared Image with Distortions

A set of 55 distorted images were generated and the JB goodness of fit calculation was run on the set of distorted images. As expected, distortions impact the regularity and fit of the MSCN. Interestingly enough, some distortions actually improved the fit and resulted in better JB scores than the original image. In reviewing the original image, it had a little blur on the edges and had some over exposed areas which gave it a higher JB value to start with. Table 3 has a summary of the JB scores for a single image with a variety of distortions.

Image	# of images	Average JB of MSCN	Median JB of MSCN	Min JB of MSCN	Max JB of MSCN
Indoor IR Distorted (single image all distortions)	55	139.85	80.72	3.38	407.85

Table 3: Average Fit for Sample Distorted IR Images

APPLICATION TO DETECTION ALGORITHM

Imagery was used from sample over sea visual and infrared imagery. Images were taken from video sequences from a variety of times of day. Detection ground truth data was not readily available so it had to be extracted from log information containing detection times which were then matched to time stamped image frames. In order to have a more manageable data set, imagery from the video sequences was down-sampled to 1 in every 100 frames. Due to the limited scope and time of this project, the ground truth data was limited to categorizing detections and missed detections and all frames without detections were removed from the dataset. A detection is defined as a frame that the algorithm marked as having a detection. A missed detection is defined as a frame which the algorithm did not mark as having a detection but visually, a human could see in the imagery (both visual and IR) that an object of interest was present.

For all features, the Spearman's rank ordered correlation coefficient was calculated in order to determine the strength of the relationship between the quality features and missed detections. The correlation between the quality measures was lower than expected, and not significant enough in order to be able to predict conditions when false negative detections may occur. As shown in Figure 22, all SROCC values were below 0.5 for the infrared imagery. In the first 18 features, there generally are weaker relationships than in the last 18 features. In BRISQUE, the second set of features use the image at half the scale.

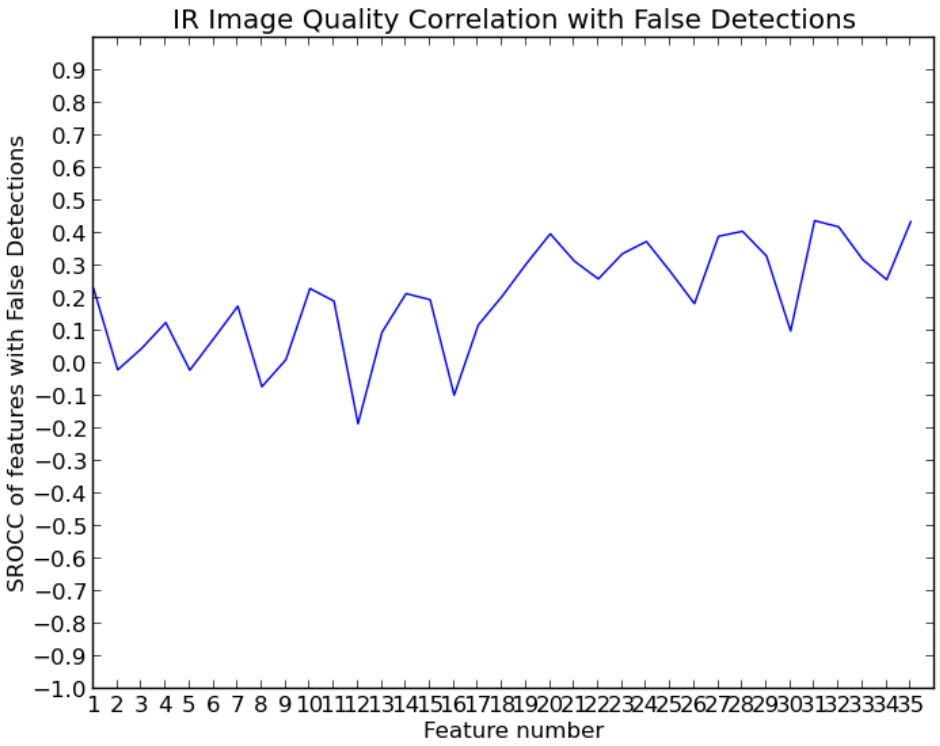

Figure 22: SROCC of Infrared Features with Missed Detections

When analyzing the correlation between missed detections in visual images, there is an even weaker relationship. Figure 23 shows the graph of features to SROCC values for the visual imagery. There is virtually no correlation in the first 18 features; However in the second 18 features, there is slight correlation with the maximum being 0.34.

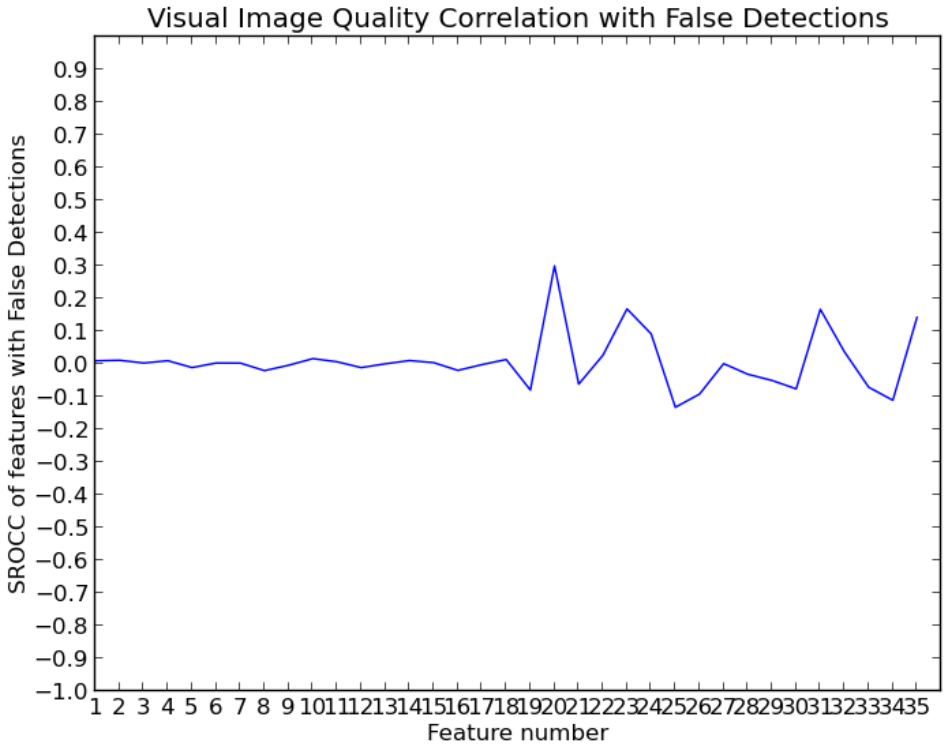

Figure 23: SROCC of Visual Features with Missed Detections

The lack of correlation between the quality features could be due to various reasons. After reviewing the detection images more closely, at appears that the perceived overall quality of the images which BRISQUE is designed to predict may be considered very similar, especially for the visual images. This may also contribute to the lack of strong relationship between false detections and BRISQUE quality features. For the sample data, the algorithm may not be as sensitive to the quality defects that the BRISQUE algorithm measures. Missed detections could also be due to various other problems in the imagery not detected by BRISQUE such as issues with shape of objects. The detection algorithm also requires a certain amount of calibration and training and there could have been problems in training the detection algorithm to the missed targets.

The stronger correlation in the infrared imagery may suggest that this particular detection algorithm is more dependent on having quality infrared imagery.

Chapter 5

Discussion

Overall, the quality features of the BRISQUE image quality algorithm as applied to infrared images was shown to have similar properties and profiles as visual images. Indoor and outdoor infrared images varied slightly. Based on the observations, BRISQUE could be useful in measuring image quality since infrared images share similar statistical regularities in the BRISQUE feature metrics.

The application of the utilizing the BRISQUE algorithm to determine when false detections are present did not have strong enough correlation to be relevant. Future research in this area to further establish the applicability of BRISQUE for use in quality of infrared images would be to conduct a human survey of the infrared images dataset and generate DMOS scores to perform the same analysis done in the original BRISQUE paper. Additionally, the images used for detection could be further analyzed to determine if there is uniqueness in the quality features of the image sets with detections and missed detections. A different approach could also be to use the detection algorithm and inject image defects into the image set to degrade the performance of the algorithm and then run the images through the algorithm again to determine the point at which poor quality causes problems in the algorithm. Another approach would be to utilize an algorithm which may specifically be impacted by noise and or blur in order to validate application of the algorithm to infrared imagery.

References

[1] Mittal, A.; Moorthy, A.K.; Bovik, A.C., "No-Reference Image Quality Assessment in the Spatial Domain," *Image Processing, IEEE Transactions on* , vol.21, no.12, pp.4695,4708, Dec. 2012.

[2] Morris, N.J.W.; Avidan, S.; Matusik, W.; Pfister, H., "Statistics of Infrared Images," *Computer Vision and Pattern Recognition, 2007. CVPR '07. IEEE Conference on*, vol., no., pp.1,7, 17-22 June 2007.

[3] Yin Chen; Genshe Chen; Blum, R.S.; Blasch, E.; Lynch, R.S., "Image Quality Measures for Predicting Automatic Target Recognition Performance," *Aerospace Conference, 2008 IEEE* , vol., no., pp.1,9, 1-8 March 2008.

[4] Rouse, D.M.; Hemami, S.S., "Natural image utility assessment using image contours," *Image Processing (ICIP), 2009 16th IEEE International Conference on*, vol., no., pp.2217,2220, 7-10 Nov. 2009.

[5] A. C. Bovik, Handbook of Image and Video Processing. New York: Academic, 2005.

[6] A. Srivastava, A. B. Lee, E. P. Simoncelli, and S. C. Zhu, "On Advances in Statistical Modeling of Natural Images," *J. Math. Imag. Vis*, vol. 18, no. 1, pp. 17-33, 2003.

[7] Huixuan Tang; Joshi, N.; Kapoor, A., "Learning a blind measure of perceptual image quality," *Computer Vision and Pattern Recognition (CVPR), 2011 IEEE Conference on* , vol., no., pp.305,312, 20-25 June 2011

[8] Peng Ye; Doermann, D., "No-reference image quality assessment based on visual codebook," *Image Processing (ICIP), 2011 18th IEEE International Conference on*, vol., no., pp.3089,3092, 11-14 Sept. 2011

[9] Saad, M.A.; Bovik, A.C.; Charrier, C., "DCT statistics model-based blind image quality assessment," *Image Processing (ICIP), 2011 18th IEEE International Conference on*, vol., no., pp.3093,3096, 11-14 Sept. 2011

[10] Moorthy, A.K.; Bovik, A.C., "Blind Image Quality Assessment: From Natural Scene Statistics to Perceptual Quality," *Image Processing, IEEE Transactions on*, vol.20, no.12, pp.3350,3364, Dec. 2011.

[11] Sheikh, H.R.; Bovik, A.C.; de Veciana, G., "An information fidelity criterion for image quality assessment using natural scene statistics," *Image Processing, IEEE Transactions on*, vol.14, no.12, pp.2117,2128, Dec. 2005.

[12] Narvekar, N.D.; Karam, L.J., "A no-reference perceptual image sharpness metric based on a cumulative probability of blur detection," *Quality of Multimedia Experience, 2009. QoMEx 2009. International Workshop on*, vol., no., pp.87,91, 29-31 July 2009.

[13] Ferzli, R.; Karam, L.J., "A No-Reference Objective Image Sharpness Metric Based on the Notion of Just Noticeable Blur (JNB)," *Image Processing, IEEE Transactions on*, vol.18, no.4, pp.717,728, April 2009.

[14] J. López-Alonso, J. Alda, and E. Bernabéu, "Principal-Component Characterization of Noise for Infrared Images," Appl. Opt. **41**, 320-331 (2002).

[15] Zhang Chang-jiang; Fan Yang; Xiao-Dong Wang; Hao-Ran Zhang, "An efficient non-linear algorithm for contrast enhancement of infrared image," *Machine Learning and Cybernetics, 2005. Proceedings of 2005 International Conference on*, vol.8, no., pp.4946,4951 Vol. 8, 18-21 Aug. 2005.

[16] Bing-jian Wang, Shang-qian Liu, Qing Li, Hui-xin Zhou, "A real-time contrast enhancement algorithm for infrared images based on plateau histogram", *Infrared Physics & Technology*, Volume 48, Issue 1, April 2006, Pages 77-82, ISSN 1350-4495, http://dx.doi.org/10.1016/j.infrared.2005.04.008.

[17] John M. Irvine; "National imagery interpretability rating scales (NIIRS): overview and methodology". Proc. SPIE 3128, Airborne Reconnaissance XXI, 93 (November 21, 1997).

[18] Rouse, D.M.; Hemami, S.S., "Natural image utility assessment using image contours," *Image Processing (ICIP), 2009 16th IEEE International Conference on*, vol., no., pp.2217,2220, 7-10 Nov. 2009.

[19] Zhijie Zhang ; Jufeng Zhang ; Song Yue ; Chensheng Wang; "Infrared image quality assessment based on fractal dimension method." Proc. SPIE 8562, Infrared, Millimeter-Wave, and Terahertz Technologies II, 856220 (December 5, 2012).

[20] Jianfeng Long; Shutao Li, "Near Infrared Face Image Quality Assessment System of Video Sequences," *Image and Graphics (ICIG), 2011 Sixth International Conference on* , vol., no., pp.275,279, 12-15 Aug. 2011.

[21] W.-H. Diao, X. Mao, and V. Gui, "Metrics for performance evaluation of preprocessing algorithms in infrared small target images," *Progress In Electromagnetics Research*, Vol. 115, 35-53, 2011.

[22] Peng Wang ; Ji-yin Sun ; Xi-nuo Ju; "FLIR image quality assessment for gray scale template matching." Proc. SPIE 8003, MIPPR 2011: Automatic Target Recognition and Image Analysis, 800317 (December 08, 2011).

[23] Yin Chen; Genshe Chen; Blum, R.S.; Blasch, E.; Lynch, R.S., "Image Quality Measures for Predicting Automatic Target Recognition Performance," *Aerospace Conference, 2008 IEEE* , vol., no., pp.1,9, 1-8 March 2008.